Wind Tunnel and Flight Performance of the YF-12 Inlet System

Donald B. Smeltzer*
NASA Ames Research Center, Moffett Field, Calif.
and
Ronald H. Smith†
NASA Flight Research Center, Edwards, Calif.
and
Robert W. Cubbison*
NASA Lewis Research Center, Cleveland, Ohio

The steady-state internal performance from ⅓-scale and full-scale wind tunnel models of the YF-12 inlet system is compared with results from flight tests. All systems were thoroughly instrumented for static and total pressure measurements. Results obtained included the inlet mass flows, surface pressure distributions, boundary-layer profiles, and detailed total pressure measurements at the engine face. Inlet performance is compared at Mach numbers 2.1 and 2.8 and at several Reynolds numbers over a wide range of inlet operating conditions. The data generally show good agreement between the three systems when inlet conditions are closely matched.

Nomenclature

A	= area
DPR'	= duct pressure ratio, average of two static pressures near the shock trap divided by the spike tip pitot pressure
h	= local height normal to the inlet surface
M	= Mach number
m	= mass flow
p	= static pressure
p_p	= pitot pressure
p_t	= total pressure
$\bar{p}_t$	= average total pressure
$\frac{p_{t_{2\max}} - p_{t_{2\min}}}{\bar{p}_{t_2}}$	= engine face distortion
R	= capture radius
Re	= Reynolds number based on ⅓-scale inlet diam = 1.0
X_{cowl}	= station relative to the cowl lip
α	= angle of attack
β	= angle of sideslip

Superscripts

abp	= aft bypass
c	= capture
cb	= centerbody
fbp	= forward bypass
max	= maximum
min	= minimum
st	= shock trap
x	= local
2	= engine face
∞	= freestream

Introduction

THE problems inherent in using wind tunnel test results from inlet models to predict flight performance have not been resolved satisfactorily, partially because all conditions found in flight cannot be simultaneously duplicated in the wind tunnel. For example, if relatively small models with forebodies are tested, thus creating the proper flowfield entering the inlet, flight Reynolds numbers will not be achieved. Conversely, if large-scale isolated inlets are tested, any nonuniform flowfield found in flight will not be duplicated.

To answer these questions and to provide a sound data base for comparing results between flight and scaled models, a comprehensive program involving wind tunnel and flight tests of the YF-12 inlet system was undertaken. The principal objective was to develop methods for the extrapolation of the inlet dynamic performance characteristics from wind tunnel to flight. Secondarily, the objectives were to determine the sensitivity of the systems to variables such as scale, Reynolds number, and flowfield entering the inlet. Development of methods for the extrapolation of dynamic results from wind tunnel to flight is considered to depend on good correlation of steady-state performance. This steady-state correlation is based on factors such as pressure recovery and distortion at the engine face and the main and auxiliary inlet mass flows. This paper is addressed to the correlation of these steady-state parameters between wind tunnel and flight. In addition, the effects of Reynolds number and local flowfield entering the inlet are discussed.

One-third and full-scale YF-12 inlet models were tested in wind tunnels and the performance of the YF-12 inlet system was measured in flight. All systems were thoroughly instrumented for both steady-state and dynamic total and static pressures. From these measurements the steady-state pressure recovery and distortion at the engine fact, the main and auxiliary mass flows, and boundary-layer profiles along both walls were determined. This paper gives representative steady-state performance comparisons at Mach numbers 2.1 and 2.8. References 1–6 give other steady-state and dynamic results from the wind tunnel and flight tests. Analysis of dynamic data is in progress and is expected to be reported in the near future.

YF-12 Aircraft

A photograph of the YF-12 airplane is shown in Fig. 1. The YF-12 is a two-place, twin engine interceptor capable of operation at high altitudes and Mach numbers. The inlets are of the mixed compression axisymmetric type mounted approximately at the midspan of each wing.

Comparison of the Three Test Systems

A comparison of the three inlet systems, together with the program objectives, is shown in Fig. 2. The 1/3-scale inlet was tested in the 8×7, 9×7, and 11×11 ft sections of the Ames

Received July 1, 1974; presented as Paper 74-621 at the AIAA 8th Aerodynamic Testing Conference, Bethesda, Maryland, July 8–10, 1974; revision received September 19, 1974.
Index category: Airbreathing Propulsion, Subsonic and Supersonic.
* Research Scientist.
† Research Scientist. Member AIAA.

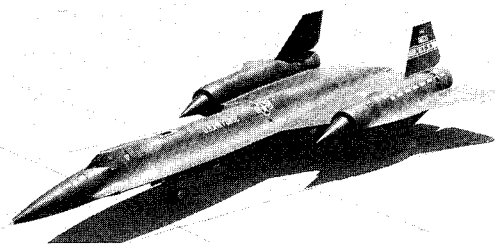

Fig. 1 Photograph of the YF-12 airplane.

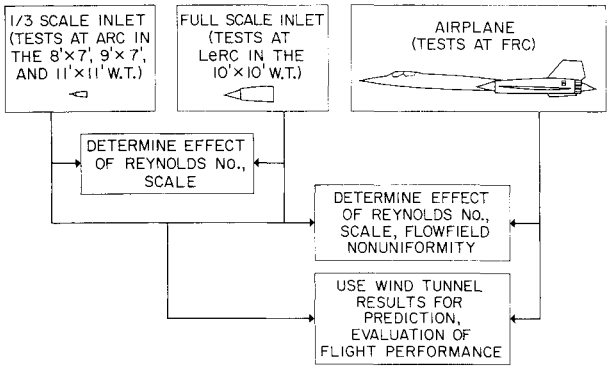

Fig. 2 Scope of the investigation and program objectives.

Research Center Unitary Plan Wind Tunnels. The full-scale inlet was tested in the 10 × 10 ft wind tunnel at Lewis Research Center. Flight tests of the inlet system of the YF-12 airplane were conducted at Flight Research Center. The effects of Reynolds number and scale were determined from the 1/3- and full-scale wind tunnel tests. Also, these results were compared with results from flight tests to determine the effect of flowfield nonuniformity. Ultimately, steady-state, and dynamic results from the wind tunnel tests will be used to predict flight performance, and these predictions will be compared to the inlet performance measured in flight.

Details of the 1/3- and Full-Scale Inlets

Details of the 1/3- and full-scale inlets are shown in Fig. 3. All systems have the same internal contours and employ a translating centerbody for control of the throat area. Porous bleed (slots) is provided for boundary-layer control on the centerbody. Each system has a combination ram scoop/flush slot called a "shock trap" for boundary-layer control on the cowl. An aft bypass system is used for inlet-engine airflow matching for off-design operation. All systems have a forward bypass, which is normally used on the airplane for control of the position of the terminal shock wave. The areas of both bypass systems are varied by using rotary valves.

A duct pressure ratio (*DPR'*) was measured for the three inlet systems at all inlet operating conditions. This quantity is an indication of the relative position of the terminal shock wave and was obtained from the average of two static pressures located on the cowl just downstream from the shock trap divided by the spike tip pitot pressure. The static pressures were at the same axial location but were 180° apart. *DPR'* was thought to be a unique measurement that defined a particular performance level at each Mach number. However, this was not the case at Mach number 2.1, as will be discussed later.

There were some differences in the geometry of the three systems. Both wind tunnel models had a cold pipe and flow control plug downstream of the engine face. These items, of course, were not used in flight. Also, on the full-scale inlet and in flight, the centerbody bleed and forward bypass mass flows are ducted to the freestream through fixed flush louvers. On the 1/3- scale inlet, however, these flows were

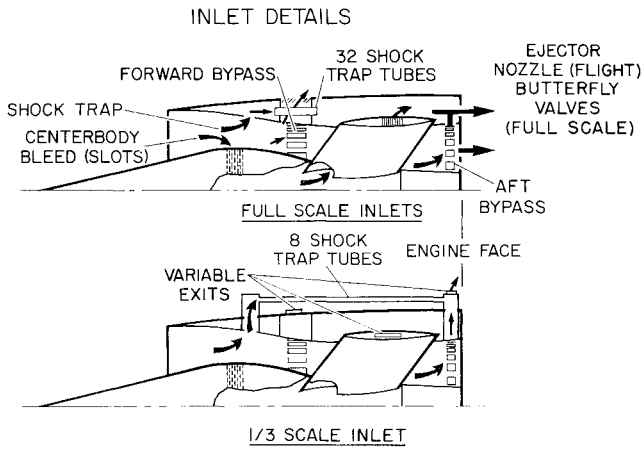

Fig. 3 Details of the full-scale and 1/3-scale inlet systems.

ducted to the freestream through variable exits so that the mass flows could be matched with that of the other systems. For the full-scale and flight inlets, the shock trap flow is ducted across the forward bypass plenum through 32 shock trap tubes, mixed with the aft bypass flow and, in flight, exited through the ejector nozzle for engine cooling. However, an engine was not used for the full-scale wind tunnel tests. Instead, butterfly valves were used for the control of these combined flows. For the 1/3-scale inlet, the 32 shock trap tubes were simulated by 8 area-scaled tubes. The combined flows were then removed through a variable exit. The effect of this simulation will be discussed later. Further details of the flight hardware are given in Refs. 1 and 2.

Airplane Flowfield Nonuniformity

In flight, the inlet entrance is in a nonuniform flowfield. The elements on the airplane that contribute to this nonuniformity are shown in the lower half of Fig. 4. Weak shock waves are shown to originate from the canopy, antenna, doors, and chines. These shock waves intersect the conical flowfield ahead of the inlet entrance, creating nonuniformity in both the flow angle and Mach number. The result for one set of freestream conditions is the flowfield shown in the upper half of the figure.‡ The data were obtained at the *plane* of the cowl lip with the inlet *removed*. The freestream Mach number (2.75), angle-of-attack (5.3°), and angle of sideslip (0°) are shown.§ The flowfield survey shows that the Mach number ranges from 2.73 to 2.80 at the cowl lip radius and from 2.74 to 2.81 in the same plane at the centerbody radius. The inlet is well aligned with ±1° in the angle-of-attack plane while the angle of sideslip is not as uniform since it ranges between +2° and −4°. The results in the angle of sideslip plane would seem to indicate vortex flow. It should be emphasized that these data were obtained from a 1/12-scale model with the inlet *removed* —the presence of a conical centerbody could modify these results.

Instrumentation of the Three Inlet Systems

Instrumentation details are shown in Fig. 5. The inlets have steady-state and dynamic instrumentation at the locations indicated by the letters *A* through *F*. The forward portion of the centerbody is represented by *A*, the forward cowl by *B*. The aft cowl and centerbody are represented by *C* and *D*, respectively. Measurements in the various mass flow plenums are represented by *E*, and the engine face is represented by *F*.

‡ These data are unpublished results from a wind tunnel survey of the YF-12 flowfield at the plane of the cowl lip. The data are available from J. Gawienowski at Ames Research Center.

§ The freestream angle of attack is close to the angle between the fuselage reference plane and the inlet centerline, thereby aligning the inlet with the freestream.

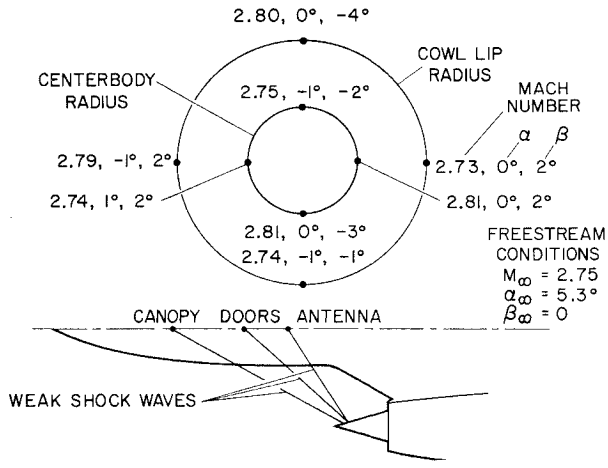

Fig. 4 Airplane geometry causing a nonuniform flowfield at the cowl lip.

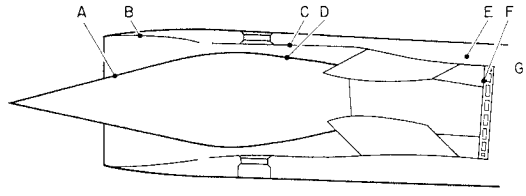

NASA RESEARCH CENTER	SCALE	TYPE	LOCATION OF PRESSURE SENSORS A	B	C	D	E	F	G	TOTAL
			NUMBER OF SENSORS							
AMES	1/3	STEADY STATE	73	32	84	44	47	40	—	320
		DYNAMIC	12	6	16	12	1	40	—	87
LEWIS	FULL	STEADY STATE	75	58	128	94	45	52	—	402
		DYNAMIC	—	11	27	—	12	24	—	74
FLIGHT	FULL	STEADY STATE	9	17	43	22	7	50	3	151
		DYNAMIC	4	4	8	8	5	46	5	80

Fig. 5 Summary of instrumentation for the wind tunnel and flight tests.

Engine measurements made in flight are represented by *G*. The instrumentation included conventional tubes and orifices for the steady-state measurements and high response cells for the dynamic instrumentation.

Results and Discussion

Performance Comparisons at Mach Number 2.8

The principal performance comparisons are presented in terms of pressure recovery at the engine face vs the various inlet mass flow ratios. These comparisons are shown in Fig. 6 for Mach number 2.8. The data were obtained by varying the forward bypass door—the control used in flight for positioning the terminal shock wave. The trend in pressure recovery with mass flow at the engine face agrees quite well for the three inlets.[¶] However, in flight, the inlet remained started to a higher pressure recovery than it did for either wind tunnel model in spite of the fact that, in flight, the inlet operates in a nonuniform flowfield.[**] The recovery was somewhat low for the 1/3-scale inlet, possibly because of the low Reynolds number for the 1/3-scale tests. The direct effect of Reynolds number on the 1/3-scale inlet performance will be discussed later. The trend of pressure recovery with shock trap flow is similar for the wind tunnel models but is different in flight. There are possible reasons for this. In flight, the engine acts as a pump on this passage, thus possibly modifying the flow characteristics. Additionally, the shock trap/aft bypass coupling is different for the three inlets, producing an effect that is discussed later. The centerbody bleed flows are comparable for the two wind tunnel models. However, this flow is somewhat higher in flight. The centerbody system of the flight hardware is known to leak which would tend to increase the measured centerbody bleed.[††]

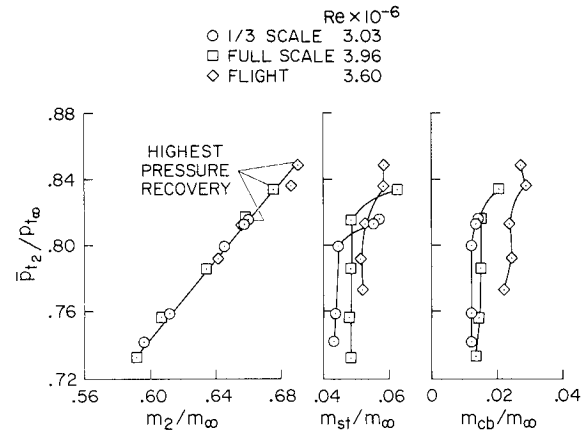

Fig. 6 Mass flows of the three inlet systems at Mach number 2.8.

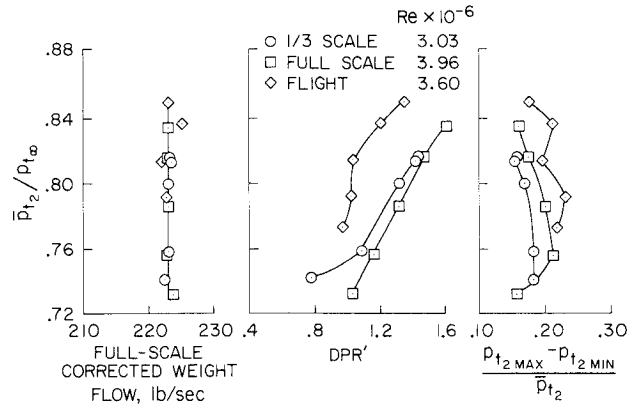

Fig. 7 Additional performance at Mach number 2.8.

Other performance parameters at Mach number 2.8 are shown in Fig. 7. Since mass flow vs pressure recovery at the engine face was in good agreement for the three systems, naturally the full-scale corrected weight flows vs pressure recovery are in good agreement. The trend of duct pressure ratio vs pressure recovery is different for the three inlets, particularly the flight results. Duct pressure ratio was supposed to be an indication of the relative terminal shock wave position, but this may not be the case.[‡‡] The comparison of the distortion at the engine face vs pressure recovery is considered good since distortion is sensitive to the maximum or minimum total pressure measurement.

[¶] These curves correspond to data obtained for a constant corrected engine airflow.

[**] The flight results are dependent on the total pressure at the inlet entrance. This is *not* the same as freestream total pressure. The local total pressure is the average of a single pitot pressure measurement made during many flights of the airplane and is subject to a greater uncertainty than is total pressure measured in the wind tunnel.

[††] The higher centerbody bleed in flight may explain the higher pressure recovery compared to the wind tunnel models. Based on experience from previous tests of axisymmetric inlets, the centerbody bleed measured in the wind tunnel is believed to be too low for good inlet performance.

[‡‡] Pressure recovery vs mass flow at the engine face was in good agreement. This should indicate similar shockwave losses and/or positions.

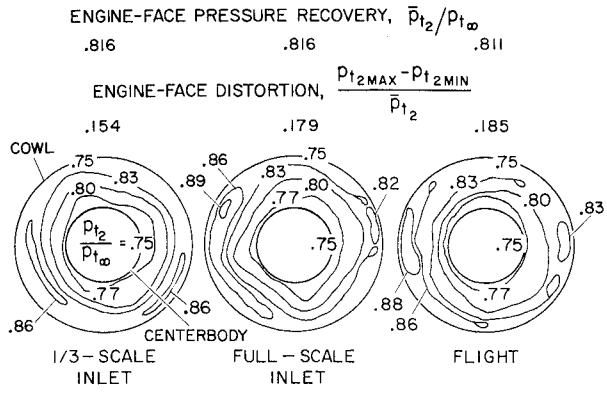

Fig. 8 Total pressure contours at the engine face, $M_\infty = 2.8$.

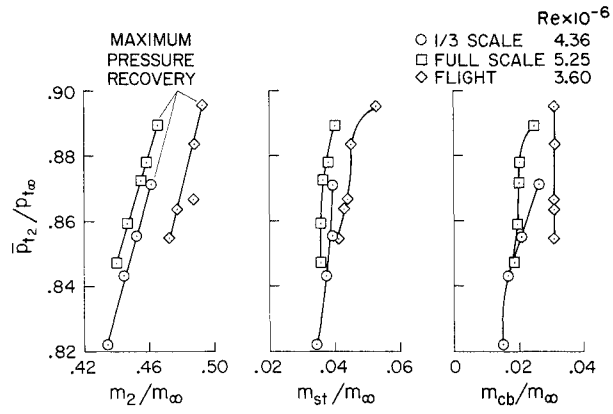

Fig. 9 Mass flows of the three inlet systems at Mach number 2.1.

Details of the total pressure patterns at the engine face are shown by the contour maps in Fig. 8. Generally, contours for the three inlets are shown at the same pressure recovery. Average values of pressure recovery and distortion are indicated above each figure. Note that the pressure recovery on both walls (surface statics) is the same for all inlets. Between the last contour shown and the cowl, the pressure recovery usually drops linerally to the value at the wall. Near the centerbody, the total pressure contours are quite similar. Near the cowl, however, there are differences, higher pressure recovery occurs for the full-scale inlet and in flight than for the 1/3-scale inlet. As a consequence, the inlets with higher pressure recovery have higher average distortion. Overall, the pattern comparison is considered good. This may enhance the possibility of good dynamic data correlation.

Performance Comparisons at Mach Number 2.1

The performance comparisons at Mach number 2.1 are based on the same parameters as at Mach number 2.8. The mass flows vs pressure recovery at the engine face are shown in Fig. 9. As at Mach number 2.8, maximum pressure recovery is highest in flight, followed by the full-scale and 1/3-scale inlets. However, the comparison of pressure recovery vs mass flow at the engine face is not as good as it was at Mach number 2.8. Better agreement would have been obtained with a different setting of the flow control plug, as will be discussed shortly. Causes of the discrepancies in the trends of pressure recovery vs the shock trap and centerbody bleed flows are the same as discussed for the results at Mach number 2.8.

Additional data at Mach number 2.1 are shown in Fig. 10. Note that the full-scale corrected weight flow is different for the three inlets. Increasing the area at the flow control plug would increase the corrected weight flow of the wind tunnel models because, at a fixed pressure recovery and freestream Mach number, corrected weight flow depends only on the area at the flow control plug (this area is always choked). The trend of duct pressure ratio vs pressure recovery at the engine face is similar for the wind tunnel models. In flight, however, the trend is different—indicating again, as at Mach number 2.8, that duct pressure ratio may not be a good indication of the relative position of the terminal shock wave. The distortion comparison is considered good for the reasons discussed at Mach number 2.8, except at the highest pressure recovery in flight. §§

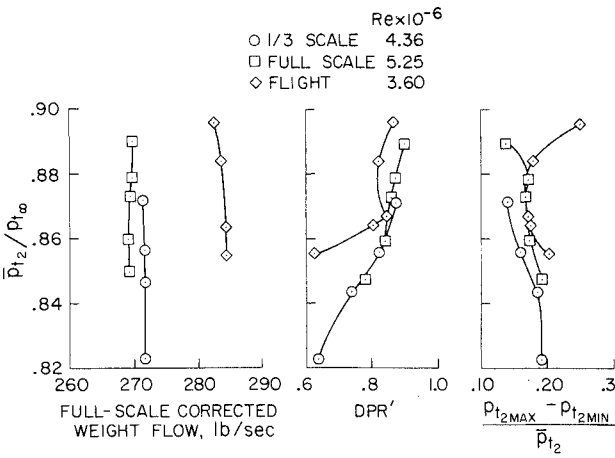

Fig. 10 Additional performance at Mach number 2.1.

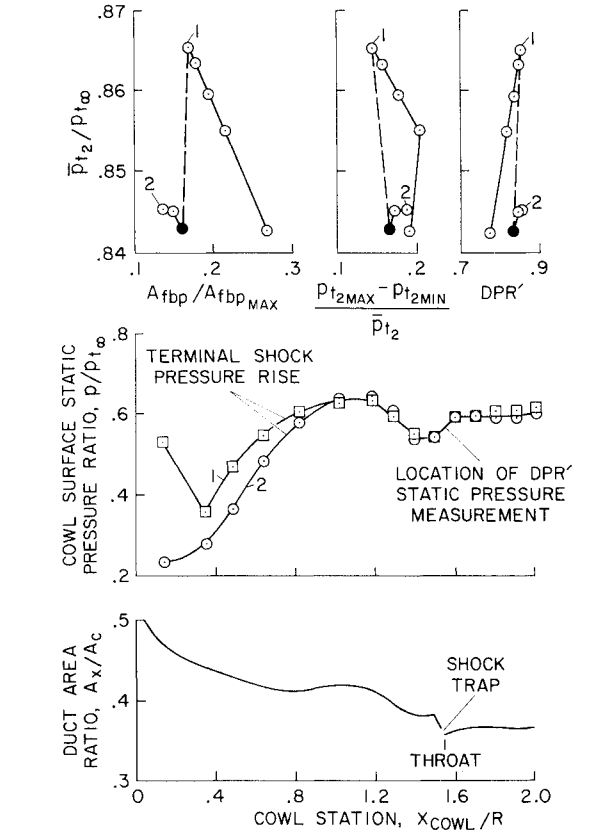

Fig. 11 Performance details from the 1/3-scale inlet at Mach number 2.1.

Performance Details at Mach Number 2.1

In flight, at about Mach number 2.1, the inlet system does not behave as a normal mixed compression inlet, since it is

§§Relatively high distortion at high pressure recovery has been observed previously during wind tunnel tests of inlet models. This combination generally occurs when the inlet is on the verge of unstarting and the terminal shock wave is relatively unstable. These conditions at high pressure recovery may not be repeatable.

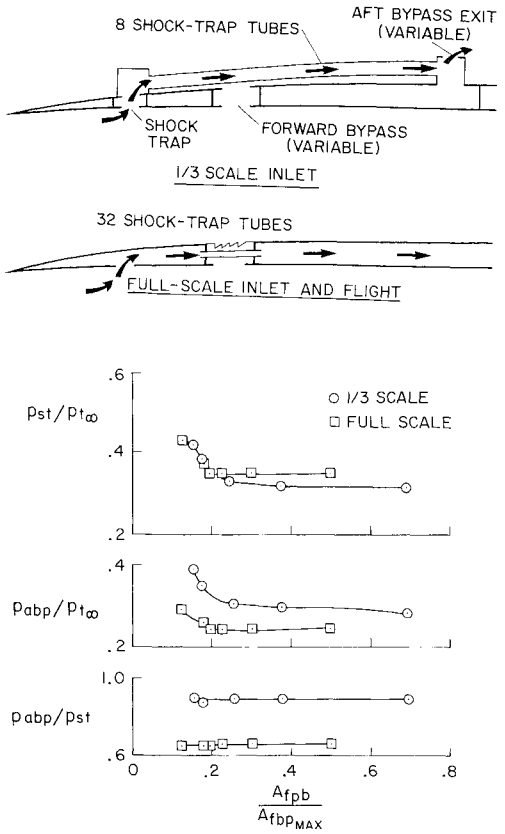

Fig. 12 Shock trap/aft bypass coupling, $M_\infty = 2.8$.

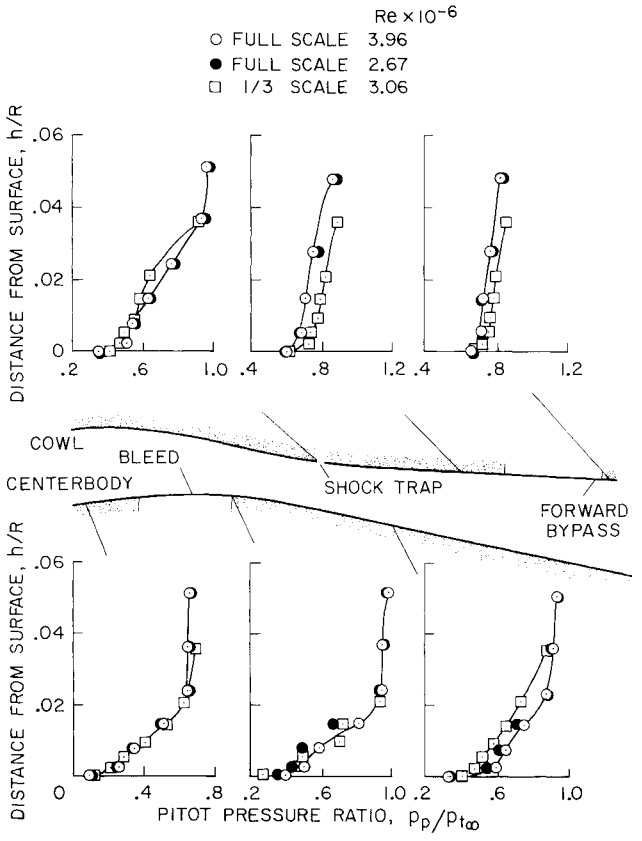

Fig. 13 Boundary-layer comparisons of the wind tunnel models at Mach number 2.8.

difficult to determine whether or not the inlet is started, based on duct pressure ratio (*DPR'*), the parameter by which the terminal shock wave is positioned. This problem was igated during the 1/3-scale inlet tests, and the results are shown in Fig.11. The position of the forward bypass door, the distortion at the engine face, and the duct pressure ratio are shown as a function of pressure recovery at the engine face on the top part of the figure. As the forward bypass door is closed, pressure recovery increases, as expected. A point is reached (point 1) where further door closing causes the pressure recovery to decrease (dashed line)—normally considered as the point of inlet unstart (filled symbol). With further door closing, pressure recovery increases slightly (point 2). Correspondingly, distortion decreases to the point of unstart and then increases as the door is closed past unstart. On the other hand, the values of *DPR'* do not change when the inlet unstarts. Obviously, then, an observer cannot rely on this *DPR'* display to determine whether or not the inlet is started.

Cowl surface pressure distributions for two conditions (points 1 and 2) with the same *DPR'* are shown in the center of the figure and the corresponding duct area distribution is shown at the bottom of the figure. Note that the surface pressures where the *DPR'* static pressure measurement is obtained are the same for the two conditions, so naturally *DPR'* does not change (see inlet details for *DPR'* definition). Also, the pressure rise through the terminal shock wave is well upstream of the throat for both conditions. This probably occurs because the duct area converges rather slowly from the cowl lip to the throat. Thus, an "aerodynamic" throat is created in the vicinity of cowl station 0.8.[¶¶]

Shock Trap/Aft Bypass Coupling

As mentioned in the discussion of performance at Mach number 2.8, the fact that the trends in shock trap flow vs pressure recovery at the engine face are different for the three inlets was possibly due to differences in the shock trap/aft bypass coupling. The effect of the different coupling is shown in Fig. 12. The sketches on the upper half of the figure indicate the differences between the 1/3-scale, full-scale, and flight hardware. Recall that the 1/3-scale inlet has a variable exit for matching the shock trap flow to that of the other inlets. The flow is set by varying the forward bypass control until *DPR'* is the same as for the full-scale inlet and in flight. The shock trap flow is then matched to that of the other two inlets by varying the aft bypass exit. Various inlet performance levels are then obtained by varying the forward bypass, the control used in flight to position the terminal shock wave. The effect of the forward bypass variation on the shock trap and aft bypass plenum chamber pressures is shown for the 1/3- and full-scale inlets on the lower half of the figure. The shock trap plenum pressure is the same for the two inlets over only a small range of forward bypass opening. Downstream, in the aft bypass plenum, the pressure is higher for the 1/3-scale inlet and, hence, the pressure ratio of aft bypass to shock trap plenum is higher for the 1/3-scale inlet. Obviously then, the coupling used for the 1/3-scale inlet—8 shock trap tubes scaled for cross-sectional area—was not a good simulation of the system used for the full-scale inlet and in flight. Since the shock trap plenum pressure and the losses through the shock trap tubes are different for the 1/3-scale inlet, the shock trap mass flow is, naturally, different.[***]

Boundary-Layer Comparisons

Pitot pressure profiles for the 1/3- and full-scale inlets are shown in Fig. 13—these measurements have not been made in flight. The sketch indicates the various rake locations—three on the centerbody and three on the cowl. Results for the full-scale inlet are shown at two Reynolds numbers (circles and

[¶¶] Current state-of-the-art indicates that supersonic flow *only* upstream of the geometric throat is best for control of the position of the terminal shock wave.

[***] In flight, an engine acts as a pump on the shock trap passage (see Fig. 3) and, therefore, might change the flow characteristics and, thus, the mass flow through this passage compared to the 1/3-scale inlet.

Table 1 Summary of the primary results

Mach Number	Model	Engine-face pressure recovery	Engine-face distortion	Engine-face mass-flow ratio	Shock-trap mass-flow ratio	Centerbody bleed mass flow ratio
2.8	1/3 scale	0.814	0.154	0.658	0.055	0.013
	full scale	0.816	0.175	0.659	0.048	0.015
	flight	0.814	0.195	0.658	0.053	0.024
2.1	1/3 scale	0.872	0.139	0.461	0.040	0.026
	full scale	0.873	0.163	0.455	0.037	0.020
	flight	0.867	0.170	0.475	0.043	0.030

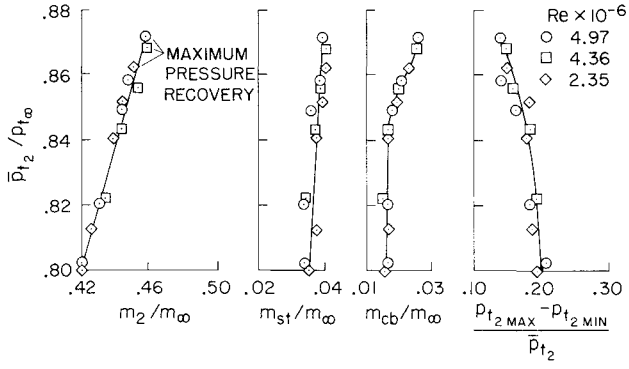

Fig. 14 Effect of Reynolds number on the 1/3-scale inlet performance at Mach number 2.1.

filled circles). Reynolds number has little or no effect on the boundary-layer development on the cowl. On the centerbody, however, the boundary layer just downstream of the bleed region is closer to separation at the lower Reynolds number, as evidenced by the lower pitot pressures near the wall (filled symbols) However these differences are less evident further downstream.

Pitot pressure comparisons between the 1/3- and full-scale inlets are good at the upstream centerbody location. However, the 1/3-scale profile just downstream of the bleed region (squares) begins to diverge slightly from the full-scale profile (circles), perhaps because the 1/3-scale bleed is slightly lower (see Fig. 5). Further downstream on the centerbody, the pitot pressures for the 1/3-scale inlet are definitely lower, although, at the outermost probe, they are the same. On the cowl, the reverse is true: the pressures are generally higher for the 1/3-scale inlet but the shape of the profiles is similar. Overall, the pitot pressure profiles are considered to be in good agreement; thus, the pressure recovery at the engine face would be expected to be about the same.

Reynolds Number Effect

As mentioned previously, the maximum pressure recovery that be achieved without unstarting the inlet may be influenced by Reynolds number. A limited amount of data were obtained at different Reynolds numbers during the 1/3-scale inlet tests. Some of the results are shown in Fig. 14 for Mach number 2.1. The various inlet mass flows and the distortion at the engine face are shown as a function of total pressure recovery at the engine face. Note that the maximum pressure recovery that can be achieved without inlet unstart increases with increasing Reynolds number. Except for this fact, the performance curves are essentially the same for all Reynolds numbers. This implies that results from inlet testing at less than a projected flight Reynolds number can be a satisfactory indication of flight performance. In fact, maximum pressure recovery in flight might be expected to be slightly higher if the flight Reynolds number is greater.

Summary of Results

A summary of the primary results at Mach numbers 2.8 and 2.1 is shown in Table 1. Data at each Mach number are shown for conditions were the total pressure recovery is nearly the same for each inlet. Distortion is comparable for the three inlets at both Mach numbers, although it is lowest for the 1/3-scale inlet and increases progressively for the full-scale inlet and in flight. The comparison of mass flow at the engine face is excellent at Mach number 2.8—at Mach number 2.1, this comparison is not as good, for reasons previously discussed. The shock trap flows compare reasonably well at both Mach numbers, although there are possible reasons for the differences (see section on shock trap/aft bypass coupling). The centerbody bleed flows compare reasonably well, even though there is leakage in the centerbody system in flight.

Conclusions

Results of wind tunnel tests of 1/3-and full-scale models of the YF-12 inlet system have been compared with results from flight tests. The performance comparisons indicate that wind tunnel results can be a satisfactory indication of performance in flight if inlet conditions are matched. Attention should be paid to geometric details in wind tunnel models. Failing this, as in the case of the shock trap/aft bypass coupling of the 1/3-scale inlet, performance comparisons may be impaired. Also, wind tunnel testing at less than flight Reynolds number does not appear to affect data comparisons seriously. Finally, in flight, no inlet performance penalties were found that could be attributed to the nonuniform flowfield. Overall, the steady-state performance comparisons are sufficient to indicate that the development of dynamic data scaling parameters for axisymmetric inlets may be possible. This comparison of the dynamic results between wind tunnel and flight is in progress and will be reported in the near future.

References

[1] Burchan, F.W., Jr., Holzman, J.F., and Reukauf, P.J., "Preliminary Results of Flight Tests of the Propulsion System of the YF-12 Airplane at Mach Numbers to 3.0," AIAA Paper 73-1314, Las Vegas, Nev., 1973.

[2] Campbell, D.H., "F-12 Series Aircraft Propulsion System Performance and Development," AIAA Paper 73-821, 1973, St. Louis, Mo.

[3] Schweikhard, W.G. and Cubbison, R.W., "Preliminary Results From Wind Tunnel and Flight Tests of the YF-12 Propulsion System," TM X-56016, 1973, NASA.

[4] Schweikhard, W.G. and Montoya, E.J., "Research Instrumentation Requirements for Flight/Wind Tunnel Tests of the YF-12 Propulsion System and Related Flight Experience," NASA paper presented at Symposium on Instrumentation for Airbreathing Propulsion, Monterey, Calif., Sept. 19–21, 1972.

[5] Johnson, H.J. and Montoya, E.J., "Local Flow Measurements at the Inlet Spike Tip of a Mach 3 Supersonic Cruise Airplane," TND-6987, 1973, NASA.

[6] Smith, R.H. and Burcham, F.W., Jr., "Instrumentation for In-Flight Determination of Steady State and Dynamic Inlet Performance in Supersonic Aircraft," NASA paper presented at Symposium on Instrumentation for Airbreathing Propulsion, Monterey, Calif., Sept. 19–21, 1972.